Makara Journal of Science

Volume 24
Issue 1 *March*

Article 6

1-24-2020

ZnO/SiO2 Composite as Catalyst for the Transformation of Glycerol to Glycerol Carbonate

Yuni Krisyuningsih Krisnandi
Department of Chemistry, Faculty of Mathematics and Science, Universitas Indonesia, Depok 16424 Indonesia, yuni.krisnandi@sci.ui.ac.id

Reinhard Eckelt
Leibniz Institut für Katalyse, LIKAT, Albert-Einstein-Str. 29 a, 18059 Rostock, Germany

Hanan Atia
Leibniz Institut für Katalyse, LIKAT, Albert-Einstein-Str. 29 a, 18059 Rostock, Germany

Martin Adam
Leibniz Institut für Katalyse, LIKAT, Albert-Einstein-Str. 29 a, 18059 Rostock, Germany

Indah Revita Saragi
Department of Chemistry, Faculty of Mathematics and Science, Universitas Indonesia, Depok 16424 Indonesia

See next page for additional authors

ZnO/SiO2 Composite as Catalyst for the Transformation of Glycerol to Glycerol Carbonate

Cover Page Footnote

Financial support from the Ministry of Education, Science, and Culture of the State Mecklenburg-Vorpommern (Germany) and LIKAT and UI Cluster Research Grant 2015 is gratefully acknowledged.

Authors

Yuni Krisyuningsih Krisnandi, Reinhard Eckelt, Hanan Atia, Martin Adam, Indah Revita Saragi, Andreas Martin, and Manfred Richter

Makara Journal of Science, 24/1 (2020), 40–49
doi: 10.7454/mss.v24i1.10741

ZnO/SiO_2 Composite as Catalyst for the Transformation of Glycerol to Glycerol Carbonate

Yuni Krisyuningsih Krisnandi[1*], Reinhard Eckelt[2], Hanan Atia[2], Martin Adam[2], Indah Revita Saragi[1], Andreas Martin[2], and Manfred Richter[2]

1. Department of Chemistry, Faculty of Mathematics and Science, Universitas Indonesia, Depok 16424 Indonesia
2. Leibniz Institut für Katalyse, LIKAT, Albert-Einstein-Str. 29 a, 18059 Rostock, Germany

[*]*E-mail: yuni.krisnandi@sci.ui.ac.id*

Received March 15, 2019 | Accepted December 19, 2019

Abstract

Zinc oxide/porous silica (ZnO/SiO_2) composite was used as a catalyst to transform glycerol to glycerol carbonate (GC), a chemical intermediate and monomer for the synthesis of new functionalized polymers. The ZnO/SiO_2 catalyst was prepared using the direct precipitation method by mixing zinc sulfate solution with Aerosil 300 silica suspension and adding potassium oxalate solution. Catalytic transformation used glycerol and urea (molar ratio = 1:1) at 140 °C, 40 mbar, and various reaction times (1–6 h). The ZnO catalyst exhibited a high percentage of glycerol conversion of 82.38%; however, the yield of GC and selectivity toward GC were relatively low (i.e., 33.33% and 40.46%, respectively). The presence of silica support ($ZnO/(x)SiO_2$ increased the selectivity toward GC and yield of GC to 74.40% to 77.83% and 57.86% to 64.30%, respectively. Furthermore, although its crystallinity decreased, the reused $ZnO/(60)SiO_2$ catalyst still exhibited a high activity. The scanning transmission electron microscopy image indicated the migration of ZnO on the surface of the composite and the possibility of ZnO-glycolate formation, which were also confirmed by FTIR measurement. Nevertheless, these results showed that ZnO/SiO_2 is a promising catalyst for the transformation of glycerol to GC.

Keywords: glycerol, glycerol carbonate, heterogeneous catalysis, ZnO/SiO_2 composite, urea

Introduction

For more than a decade, many research groups have attempted to increase the value of crude glycerol (typically containing 85% glycerol, water, and residual ester products) obtained from biodiesel production. Corma et al. [1] reviewed possible reaction routes for the utilization of glycerol as a starting material for various more valuable compounds. Some of the routes are etherification of glycerol to diglycerol and polyglycerols [1–5], oxidation of glycerol to dihydroxyacetone, dehydration of glycerol to acrolein [6,7], and preparation of glycerol carbonate (GC) [8–13].

GC is a chemical intermediate and monomer that could be used to synthesize new functionalized polymers with possible exciting applications. Magniont et al. [14] reported that, by incorporating GC into an alternative binder composed of hydraulic lime and metakaolin, new properties, such as rapid hardening, improved compressive strength, and less shrinkage, are achieved in an innovative pozzolanic matrix. Another example of new GC-derived material is glycerylic cyclocarbonic fatty acid esters, which, by promoting superhydrophilicity, could act as a surfactant and an antimicrobial [15].

Many research groups have reported the transformation of glycerol to GC using various catalysts, sources of carbonyl groups, and reaction conditions [14–17]. Carbonylation of glycerol with ethylene carbonate in supercritical carbon dioxide (CO_2) in the presence of zeolites and Amberlyst A26 (OH^- and HCO_3^- forms of ion exchange resins) resulted in a low percentage of glycerol conversion of <25% [14]. The preparation of GC using urea as the carbonyl source and catalyst with Lewis acid sites associated with sulfonate groups of the polystyrene matrix was shown to be a more feasible route [18,19], exhibiting GC molar yields of 61% to 85% based on glycerol. Yoo et al. [16] reported that the use of heterogeneous mesoporous zinc sulfate as a catalyst for the glycerol–urea reaction exhibited a good molar yield of 86%. Aresta et al. [17] investigated the role of catalyst, solvent, and reaction condition in the carboxylation of glycerol to GC using CO_2. They also reported the synthesis of GC via a reaction between glycerol and urea [17]. Lipase-catalyzed synthesis of

GC through transesterification of glycerol and dimethyl carbonate was also reported [20]. Climent et al. reported the synthesis of GC by transesterification and carbonylation using urea and hydrotalcite catalysts [21]. Wang et al. [22] reported the use of a series of lanthanum oxides as solid base catalysts for the synthesis of GC from the same starting materials. In summary, heterogeneous catalysis for the synthesis of GC from glycerol and urea (the reaction mechanism is shown in Figure 1) has drawn considerable attention particularly because both starting materials are abundant and inexpensive. In addition, the reaction step could be extended to the fixation of CO_2 because ammonia reacts with CO_2 to produce urea [17]. Therefore, this reaction mechanism has made the transformation of glycerol more attractive.

Zinc compounds, such as $ZnSO_4$ and Zn-doped ZSM-5, were previously compared with various metallic compounds, including gold-doped ZSM-5, as catalysts in the glycerol–urea reaction [20], whereby the gold catalysts showed superior activity during GC production. In this work, zinc oxide/porous silica (ZnO/SiO_2) composite was proposed to be an inexpensive catalyst to substitute for gold or rare earth composites for the transformation of glycerol to GC. Various solid-state characterization techniques were utilized to obtain comprehensive information about $ZnO/(x)SiO_2$, such as morphology, phase, and interaction of the composite with the reactants and products during the reaction. The effects of the addition of silica support, reaction time, and variation in reaction conditions on glycerol conversion ($X_{Glycerol}$), molar yield (Y_{GC}), and selectivity toward GC (S_{GC}) will also be discussed.

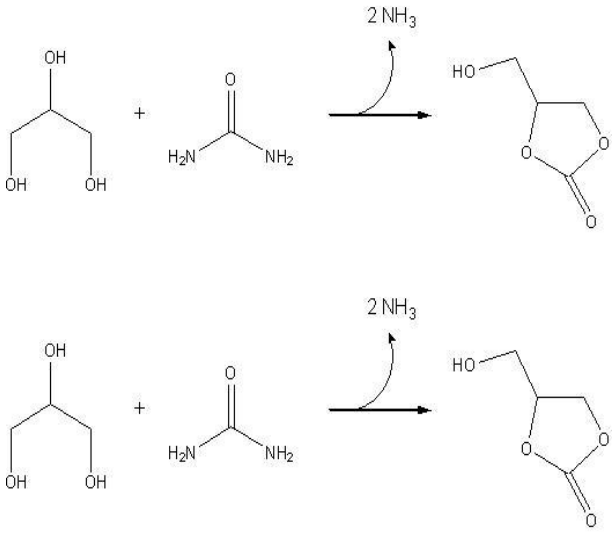

Figure 1. Reaction Mechanism of Heterogeneous Catalysis for Glycerol Carbonate (GC) Synthesis Using Glycerol and Urea as Starting Materials

Experimental

Materials. Zinc sulfate, $ZnSO_4 \cdot 7H_2O$ p.a. (Merck), potassium oxalate ($K_2C_2O_4 \cdot H_2O$) ≥ 99.9% (Sigma-Aldrich), SiO_2 Aerosil 300, glycerol (Acros), urea (Merck), and GC (TCI) were used directly without further purification.

Catalyst preparation. ZnO material was prepared using the direct precipitation method. Typically, 5.75 g $ZnSO_4$ was dissolved in 30 mL distilled water under constant stirring. At the same time, 3.685 g $K_2C_2O_4$ was dissolved separately in 30 mL distilled water. Then, the potassium oxalate solution was added to the zinc sulfate solution under vigorous stirring for another 30 min. Subsequently, the mixture was left to stand until the white precipitate of ZnC_2O_4 was observed. Finally, the product was filtered, washed with distilled water, dried at 100 °C, and calcined at 400 °C to obtain the white powder of ZnO.

ZnO/SiO_2 composite was prepared using a similar method. Prior to the addition of potassium oxalate solution at room temperature, silica suspension (Aerosil 300 with various wt%) was added to the warm $ZnSO_4$ solution (60 °C) under vigorous stirring for 30 min. The resulting zinc oxide/silica composites were labeled as $ZnO/(x)SiO_2$, in which x corresponds to the wt% of the loaded SiO_2. For the catalytic tests, the powdered catalysts were pelletized to obtain particle sizes between 315 μm and 710 μm.

Catalyst characterization. ZnO and $ZnO/(x)SiO_2$ catalysts were characterized using nitrogen adsorption BET, ICP-MS, XRD, XRF, XPS, and TEM. Surface areas and pore volumes were determined from the nitrogen adsorption isotherms at −196 °C using an ASAP 2010M characterization unit (Micromeritics). Samples were outgassed at 400 °C for 2 h under vacuum. Then, the surface area was calculated using the BET equation. Elemental analysis was conducted by ICP-OES on an OPTIMA 3000 XL spectrometer (Perkin-Elmer). The required dissolution of solids was achieved using aqua regia solution under a pressure of 8 bar according to standard routines. XRD measurements were conducted using a STADI P (STOE) setup with transmission geometry and a Ge primary monochromator with Cu Kα1 radiation. The XRD patterns were scanned in the 2θ range of 5–60 (step width = 0.58, 100 s/step) and recorded with a position-sensitive detector. The crystallite size of ZnO was determined using the Debye–Scherrer equation. Scanning transmission electron microscopy using high-angle annular dark field (STEM-HAADF) and annular bright field (STEM-ABF) were conducted with an aberration-corrected (in STEM mode, CESCOR, CEOS) microscope (JEM-ARM200F, JEOL) equipped with a 50 mm^2 Si(Li) detector (JED-2300, JEOL) for EDX analysis. For STEM-HAADF investiga-

tion, convergence angles of 30–36 mrad and an estimated spot size of 0.14 nm were used. The collection semi-angles were 90–170 mrad. For STEM-ABF investigation, the collection angle was 17 mrad with beam stopper to exclude the primary beam. The samples were prepared on a holey carbon-supported Cu or Ni grid (mesh 300) without any pretreatment.

Catalyst test and analysis. The synthesis of GC was performed following the reaction mechanism shown in Figure 1. Glycerol (typical amount of 46 g, 0.5 mol) was added to a round-bottom flask (100 mL), followed by the desired amount of urea (typical molar ratio of glycerol/urea was 1:1, unless stated in the experiment). The catalyst was added after the glycerol–urea mixture was homogeneous. Note that the amount of the catalyst was varied to keep the amount of ZnO the same for all reactions. The reaction was conducted at 140 °C, approximately 40 mbar, and various reaction times (1–6 h). The produced ammonia was pumped out under reduced pressure. The reaction products were identified and analyzed using a gas chromatograph with flame ionization detector equipped with a Chrompack FFAP 25 m × 0.32 mm × 0.3 µm column. GC from TCI was used as the reference and standard for calibration. Prior to GC measurement, the sample was diluted in distilled water to make a 1% solution.

Results and Discussion

Catalyst characterization. Powdered ZnO catalyst was prepared according to the direct precipitation method based on the metathesis reaction, followed by calcination, as shown in Equations 1 and 2:

$$2ZnSO_4{\cdot}7H_2O_{(s)} + K_2C_2O_4{\cdot}H_2O_{(s)} \rightarrow 2ZnC_2O_{4(s)} + 2K^+_{(aq)} + 2SO_4^{2-}{}_{(aq)} + 15H_2O_{(l)}, \quad (1)$$

$$ZnC_2O_{4(s)} + \tfrac{1}{2}\, O_{2(g)} \rightarrow ZnO(s) + 2CO_{2(g)}. \quad (2)$$

The as-prepared zinc oxalate, ZnC_2O_4, after being subjected to calcination at 400°C, was transformed to ZnO as the oxalic anion was decomposed into CO_2. This finding is similar to that reported by Mu et al. [23], in which oxalate from ZnC_2O_4 started to decompose at 320 °C and completely transformed to ZnO at 380 °C. In addition, the SO_4^{2-} anion was removed during filtration and washed with distilled water before calcination.

Figure 2 shows the XRD patterns of ZnO/(x)SiO_2. The ZnO particles have a wurtzite structure (hexagonal phase, space group $P63\ mc$), which is similar to the pattern reported for nanosized ZnO powder [24]. All of the diffraction peaks were attributed to the hexagonal-phase ZnO, as reported in the JCPDS card (No. 36-1451; a = 0.3249 nm, c = 0.5206 nm) [25]. The results indicate that the products consisted of pure phases and that the $ZnSO_4$ phase did not appear. Diffraction peaks related to the impurities were not observed in the XRD pattern, confirming the high purity of the synthesized product. The SiO_2 of Aerosil 300 only exhibited a broad pattern of the amorphous phase of silica, as reported by Guerfi et al. [26]. The intensity of ZnO peaks first decreased with the increase in the amount of silica support, i.e., from 30% to 50%, and then slightly increased at 60% SiO_2. The crystallite sizes of ZnO and ZnO/(x)SiO_2 catalysts, which were determined using the Scherrer equation, were in the range of 10–14 nm.

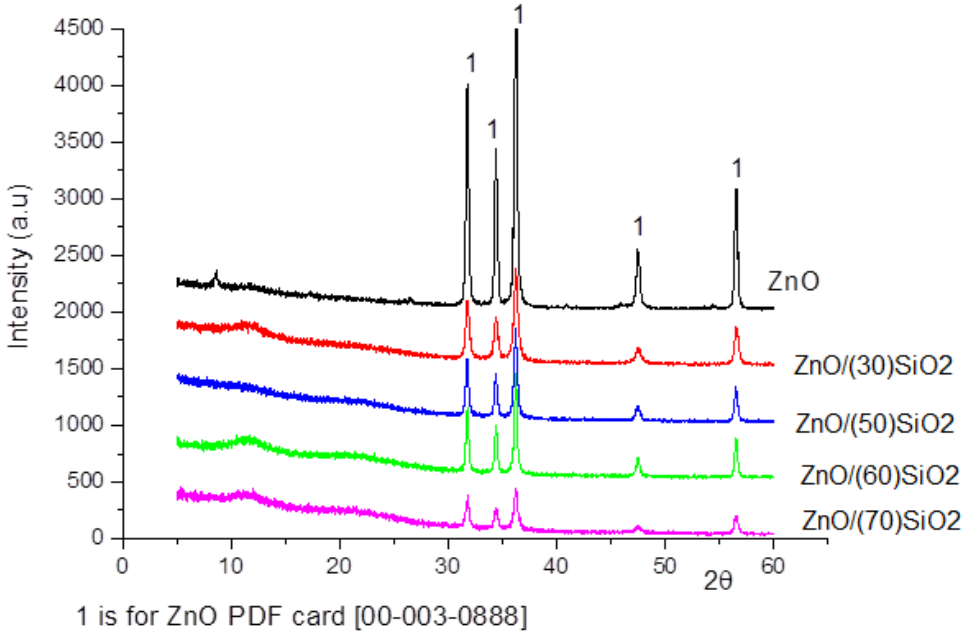

Figure 2. XRD Patterns of ZnO/(x wt%)SiO_2 Catalysts and ZnO Standard

Physicochemical analysis of the catalyst. Table 1 shows the physicochemical properties of the as-prepared ZnO and ZnO/(x)SiO$_2$ catalysts. The ICP elemental analysis shown in Table 1 indicates the decrease in Zn concentration and increase in Si concentration in the composite. The actual content of ZnO in the ZnO/(x)SiO$_2$ composites did not significantly differ from the intended amount. However, the amount of SiO$_2$ support in each composite was always lower than expected, which could be attributed to the loss of some of the SiO$_2$ support during preparation as Aerosil 300 consists of particularly fine particles. Accordingly, the specific surface area of ZnO/(x)SiO$_2$ increased with the increase in the amount of SiO$_2$ support. Furthermore, the adsorption–desorption isotherms of ZnO and ZnO/(x)SiO$_2$ composites (Figure 3) show the increase in porosity of the materials after the addition of Aerosil 300 to the system. This trend was expected when ZnO was dispersed in the finely powdered Aerosil 300. Well-dispersed ZnO in the SiO$_2$ system was also observed through STEM (see Figure 4).

STEM measurement. Figure 4 shows the electron microscopy investigation of the fresh ZnO/(60)SiO$_2$ catalyst. Notably, the ZnO particles (dark image) comprised two groups of different particle sizes, i.e., small crystals in the range of 5–10 nm (Figure 4b) and large crystals in the range of 20–50 nm (Figure 4c). The composite structure was visible in the STEM-ABF image (Figure 4d). The image contrast in the STEM-HAADF, EDX analysis (Figure 5), and XRD (Figure 2) revealed the crystals to be ZnO. SiO$_2$ exhibited an amorphous gel structure and was homogeneously distributed in the sample. Furthermore, no predominant attachment of silica to the ZnO crystals was detected. Figure 5 shows the EDX analysis of both fresh and used catalysts. The

Table 1. Physicochemical Properties of the As-prepared ZnO and ZnO/(x)SiO$_2$ Catalysts

Catalyst name	SBET [m^2/g]	Average pore diameter [nm]	Pore volume [cm^3/g]	Weight percent (ICP)			
				Zn	Si	ZnO	SiO$_2$
ZnO	17.1	8.6	0.05	83.6	–	100.0	0.0
ZnO/(70)SiO$_2$	154.4	17.8	0.82	22.7	19.2	28.3	41.1
ZnO/(60)SiO$_2$	128.1	17.0	0.67	31.0	22.3	38.6	47.7
ZnO/(50)SiO$_2$	121.8	15.4	0.58	37.8	18.0	47.0	38.5
ZnO/(30)SiO$_2$	77.3	13.3	0.34	55.4	11.8	69.0	25.2
ZnO/(60)SiO$_2$ after the reaction				32.5	7.2	40.4	15.4

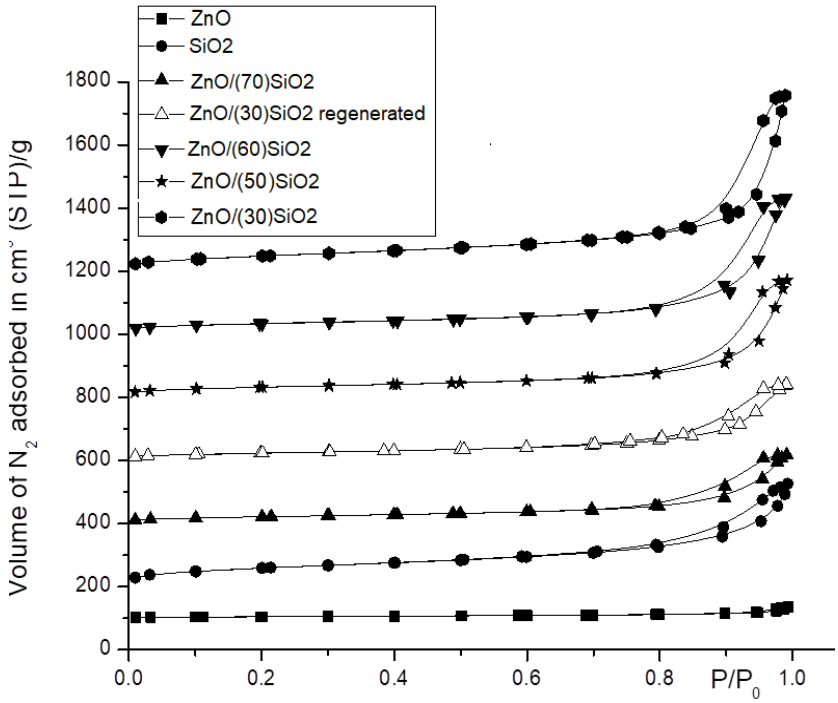

Figure 3. Adsorption–desorption Isotherms of the ZnO/(x)SiO$_2$ Composites

spectra were recorded from an area with no carbon film to exclude the resulting C signal. Figure 5a shows the STEM-HAADF image of the ZnO crystals of the fresh catalyst. The corresponding EDX spectra are marked as 1 and 2. The Cu and Ni signals arose from the TEM grids. Zn and O signals indicated a ZnO composition. In Figure 5b, a dark-field image of the used catalyst is shown. The corresponding spectrum 3 was taken from a ZnO crystal, whereas spectrum 4 was taken from the smaller morphologies shown in Figure 4b. Spectrum 4 shows a distinct carbon peak in comparison with spectrum 3 and the fresh sample (1 + 2). This distinct carbon peak might be the remainder of Zn (glycerol) after electron beam damage.

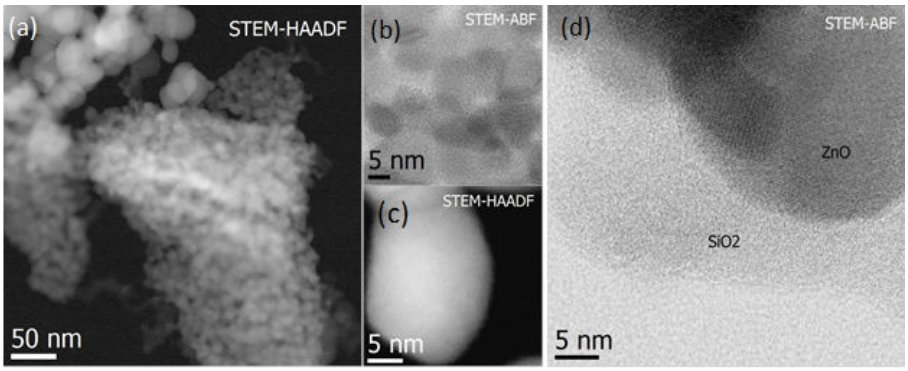

Figure 4. STEM Images of the Fresh ZnO/(60)SiO_2 Catalyst. (a) Dark-field Image of the Two Particle Sizes, (b) Bright-field Image of ZnO Crystals of 5–10 nm, (c) Dark-field Image of ZnO Crystals of 20–50 nm, and (d) Bright-field Image of ZnO Crystals and Silica

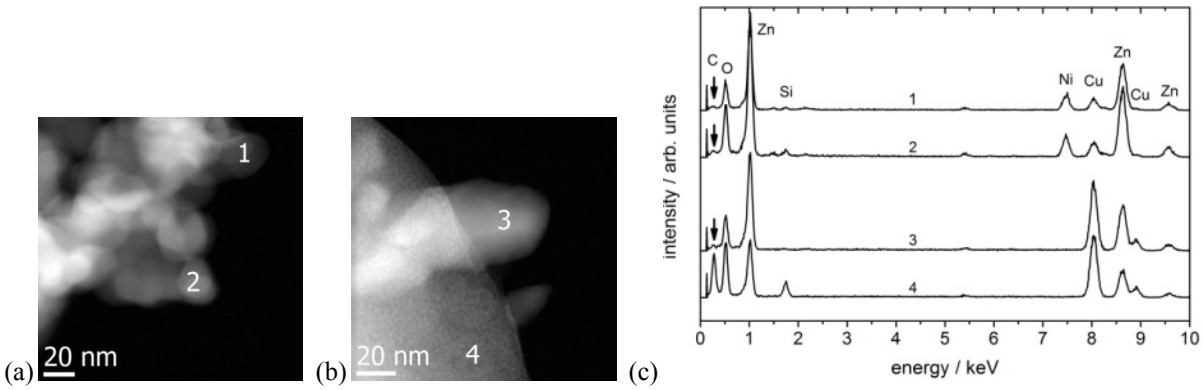

Figure 5. STEM-HAADF Images of (a) Fresh and (b) Used ZnO/(60)SiO_2 Catalysts and (c) the Corresponding EDX Analysis

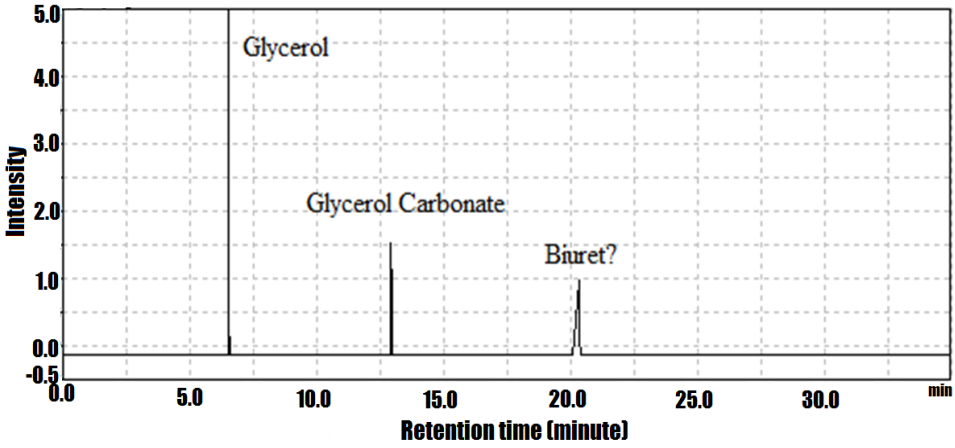

Figure 6. Chromatogram of Products from the Reaction between Glycerol and Urea Using ZnO/(40)SiO_2 Catalyst. Reaction Conditions: Glycerol/Urea Molar Ratio = 1:1, P = 30 mbar, T = 140 °C, t = 6 h

ZnO was observed to be active during the reaction. Figure 7 shows the results. $X_{Glycerol}$ was high (82.38%), but S_{GC} and Y_{GC} were low (40.46% and 33.33%, respectively). By contrast, when ZnO/(x)SiO$_2$ catalysts were used, not only $X_{Glycerol}$ but also S_{GC} and Y_{GC} increased with the increase in the amount of silica support. This finding indicates that the presence of silica support enhanced the activity of the ZnO catalyst, which can be attributed to a better distribution of the active ZnO sites in ZnO/(x)SiO$_2$, such as in ZnO/(60)SiO$_2$. Thus, the interaction between ZnO catalyst with glycerol and urea was augmented resulting in increased yield and selectivity.

Meanwhile, Hammond et al. [27] reported that the deposition of Zn, Ga, and Au onto ZSM-5 by precipitation resulted in the enhancement of GC yield, with the degree of promotion following the order: Au > Ga > Zn. The Zn-doped ZSM-5 exhibited a lower yield (<25%) than all ZnO/(x)SiO$_2$ composites in our experiment. ZSM-5 is zeolite with MFI structure, which has well-ordered pores and channels [28] and some levels of activity [29]. By contrast, Aerosil 300 has an amorphous structure, as indicated by its XRD pattern; thus, its interaction with the glycerol–urea mixture was insignificant. The characterization results showed that ZnO/(60)SiO$_2$ had the highest crystallinity and the largest surface area; its S_{GC} and Y_{GC} were also slightly higher. Therefore, ZnO/(60)SiO$_2$ was used for further experiments and was the focus of discussion in this paper.

Variation of reaction time. To obtain the optimum reaction time, four different experiments using ZnO/(60)SiO$_2$ catalyst were conducted for 1, 2, 4, and 6 h. In general, a longer reaction time results in a higher glycerol conversion and yield, as shown in Figure 8. By contrast, the percentage of selectivity toward GC (S_{GC}) increased when the reaction time was extended from 1 h to 2 h. When the reaction time was longer than 2 h, the percentage of glycerol conversion ($X_{Glycerol}$) and the percentage of selectivity toward GC (S_{GC}) were in the range of 45.8% to 45.80% and 69.67% to 77.83%, respectively. However, the percentage of GC yield (Y_{GC}) steadily increased and reached its highest value of 64.30% after 6 h. Although reactions with longer reaction times were not conducted, it could be expected that S_{GC} will not increase significantly. In addition, given that the reaction was performed in batches, unwanted side products, such as thick charcoal, could form when the reaction time was longer than 6 h. A similar phenomenon was observed in the dimerization reaction of glycerol in the presence of Cs-loaded zeolite catalysts [3].

Variation of catalyst types and conditions. Figure 9 summarizes the results of the experiments using various catalyst types and conditions. When the glycerol–urea mixture was subjected to reaction conditions without catalyst (labeled as the blank experiment), glycerol conversion still occurred ($X_{Glycerol}$ = 64.80%) but with a low Y_{GC} and S_{GC} (16.16% and 24.93%, respectively). The presence of Aerosil 300 silica in the reaction mixture caused the decrease in glycerol conversion (51.06%) but a slight increase in Y_{GC} and S_{GC} (23.58% and 44.23%, respectively). This is evidence that Aerosil 300 has a low activity toward the reaction of the glycerol–urea mixture to produce GC.

Glycerol conversion increased by 10% (from 82.61% to 92.26%) when the amount of ZnO/(60)SiO$_2$ catalyst was doubled. However, Y_{GC} and S_{GC} decreased by nearly half (from 64.30% to 45.56% and from 77.83% to 49.39%,

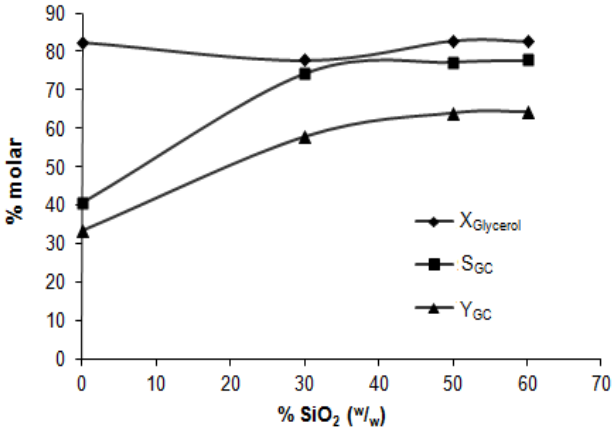

Figure 7. Results of the Reaction of Glycerol with Urea in the Presence of ZnO/(60)SiO$_2$ Catalyst as a Function of SiO$_2$ Content. Reaction Conditions: Glycerol/Urea Molar Ratio = 1:1, P = 30 mbar, T = 140 °C, t = 6 h

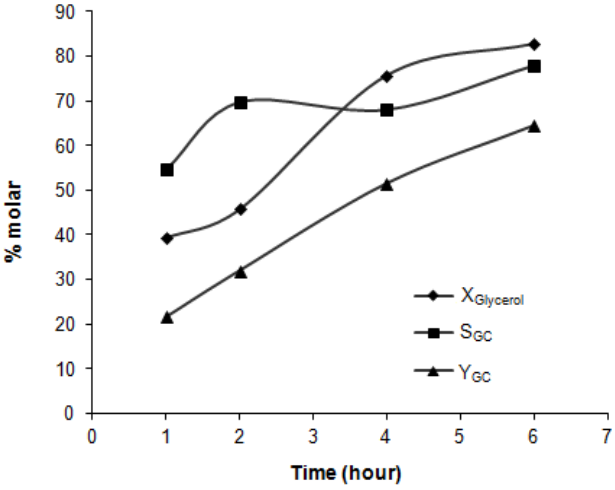

Figure 8. Results of the Reaction between Glycerol and Urea in the Presence of ZnO/(60)SiO$_2$ as a Function of Reaction Time. Reaction Conditions: Glycerol/Urea Molar Ratio = 1:1, P = 30 mbar, T = 140 °C

respectively). This finding could be attributed to excess catalyst causing further reactions to produce unwanted side products. The best catalytic performance was observed when the ratio of urea/glycerol was changed to 1.2 and the amount of the ZnO/(60)SiO_2 catalyst was maintained at 1.8 wt%, where X_{GC}, Y_{GC}, and S_{GC} reached more than 90%. This finding indicates the completion of the reaction in terms of glycerol concentration.

The effects of pressure and the use of nitrogen gas to remove the produced ammonia (NH_3) were also investigated. It is expected that nitrogen purging would induce ammonia removal and result in higher S_{GC} [30]. However, as shown in Figure 8, the conversion was lower than expected during the reaction without nitrogen purging. Furthermore, Y_{GC} and S_{GC} were similarly reduced, which could be attributed to product removal because of additional nitrogen purging. This result indicated that N_2 purging was unnecessary when the reaction was conducted at low pressure with continuous vacuum pumping. Reuse of the ZnO/(60)SiO_2 catalyst for several cycles was also investigated. Notably, the catalyst was still active, and the conversion was similar to those obtained in the reaction with fresh ZnO/(60)SiO_2 catalyst. In addition, the yield and selectivity toward GC were slightly higher. The characterization of the used catalyst showed

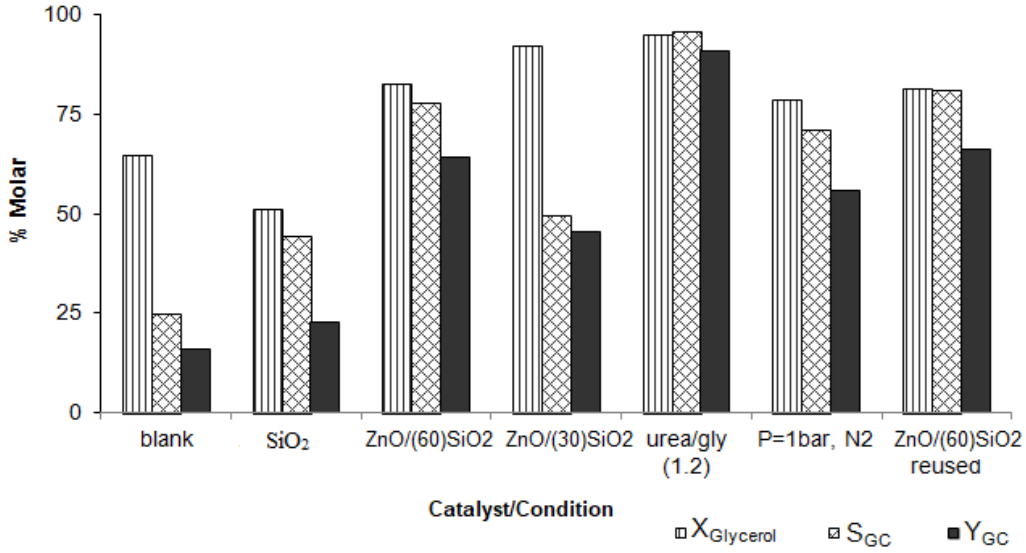

Figure 9. Comparison of Glycerol Conversion ($X_{Glycerol}$), Yield (Y_{GC}), and Selectivity Toward GC (S_{GC}) Obtained from Various Reaction Conditions

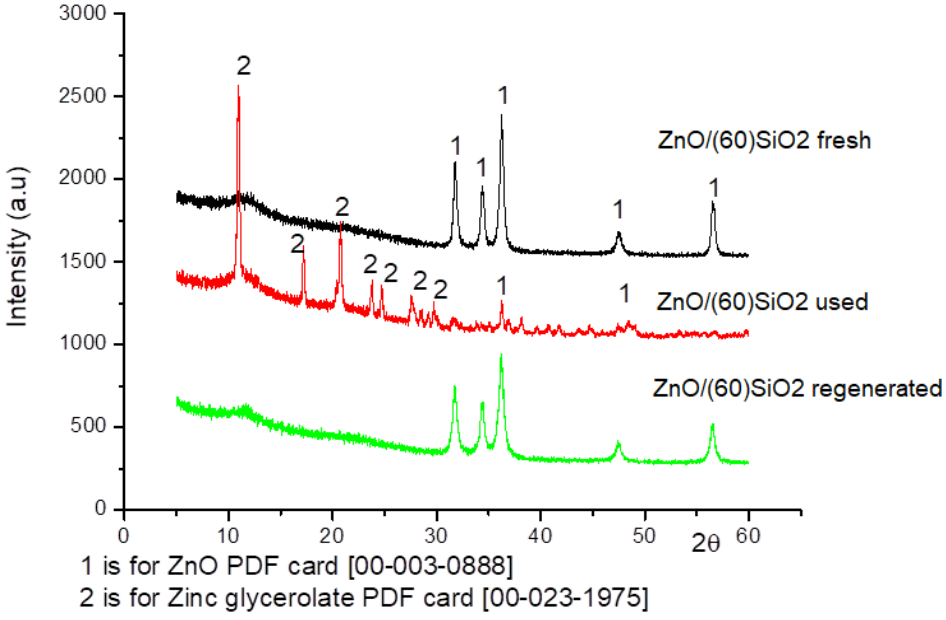

Figure 10. XRD Patterns of ZnO/(60)SiO_2

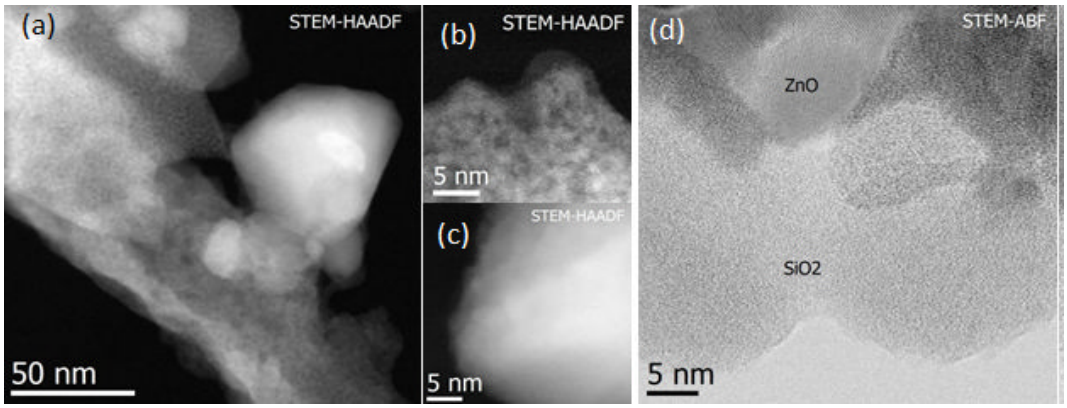

Figure 11. STEM Images of the Used ZnO/(30)SiO$_2$ Catalyst. (a) Dark-field Image as an Overview and (b) Dark-field Image with Higher Magnification of Small Particles (1–3 nm). (c) HAADF Image Showing a ZnO Cluster (Dark Gray) on the SiO$_2$ Crystal Surface (White). (d) ABF Image of the Silica and ZnO Crystals

that the Zn and Si contents were unchanged (as determined by ICP-MS, shown in Table 1). However, the XRD pattern of the used ZnO/(60)SiO$_2$ catalyst had lower peak intensities than the fresh catalyst, although the peaks of ZnO were still present (Figure 10). This finding indicates that the ZnO crystals had lost most of its crystallinity during the reaction of GC and exhibited more defects in the structure that could provide more active sites to the used ZnO/(60)SiO$_2$ catalyst. Figure 11 shows the STEM images of the used catalyst. Notably, ZnO was leaching from the composite (Figure 11c). However, overall, the morphology of the used ZnO/(60)SiO$_2$ catalyst was still similar to that of the fresh catalyst.

Conclusion

Heterogeneous catalytic reaction of the transformation of glycerol to GC using ZnO/(*x*)SiO$_2$ composite and urea as catalysts was successfully conducted. The selectivity toward GC and yield of GC were improved in the presence of porous SiO$_2$ as support, which was higher than those obtained using only ZnO catalyst. The higher the SiO$_2$ Aerosil content is, the better the values of glycerol conversion, GC yield, and selectivity toward GC.

Acknowledgments

Financial support from the Ministry of Education, Science, and Culture of the State Mecklenburg-Vorpommern (Germany) and LIKAT and UI Cluster Research Grant 2015 is gratefully acknowledged.

References

[1] Corma, A., Iborra, S., Velty, A., 2007. Chemical Routes for the Transformation of Biomass into Chemicals. American Chemical Society 107: 2411–502, https://doi: 10.1021/cr050989d.

[2] P. Guerrero-Urbaneja, C. García-Sancho, R. Moreno-Tost, J. Mérida-Robles, J. Santamaría-González, A. Jiménez-López, P.M.-T., 2014. Applied Catalysis A : General Glycerol valorization by etherification to polyglycerols by using metal oxides derived from MgFe hydrotalcites. "Applied Catalysis A, General" 470: 199–207, https://doi: 10.1016/j.apcata.2013.10.051.

[3] Krisnandi, Y.K., Eckelt, R., Schneider, M., Martin, A., Richter, M., 2008. Glycerol upgrading over zeolites by batch-reactor liquid-phase oligomerization: Heterogeneous versus homogeneous reaction. ChemSusChem, https://doi: 10.1002/cssc.200800128.

[4] Anuar, M.R., Abdullah, A.Z., Othman, M.R., 2013. Etheri fi cation of glycerol to polyglycerols over hydrotalcite catalyst prepared using a combustion method. CATCOM 32: 67–70, https://doi: 10.1016/j.catcom.2012.12.007.

[5] Bookong, P., Ruchirawat, S., Boonyarattanakalin, S., 2015. Optimization of microwave-assisted etherification of glycerol to polyglycerols by sodium carbonate as catalyst. Chemical Engineering Journal 275: 253–61, https://doi: 10.1016/j.cej.2015.04.033.

[6] Xie, Q., Li, S., Gong, R., Zheng, G., Wang, Y., Xu, P., et al., 2019. Applied Catalysis B : Environmental Microwave-assisted catalytic dehydration of glycerol for sustainable production of acrolein over a microwave absorbing catalyst. Applied Catalysis B: Environmental 243(June 2018): 455–62, https://doi: 10.1016/j.apcatb.2018. 10.058.

[7] Kiakalaieh, A.T., Aishah, N., Amin, S., 2017. Coke - tolerant SiW 20 - Al / Zr 10 catalyst for glycerol dehydration to acrolein. Chinese Journal of Catalysis 38(10): 1697–710, https://doi: 10.1016/S1872-2067(17)62891-2.

[8] Parameswaram, G., Rao, P.S.N., Srivani, A., Rao, G.N., Lingaiah, N., 2018. Magnesia-ceria mixed oxide catalysts for the selective transesterification

of glycerol to glycerol carbonate. Molecular Catalysis 451: 135–42, https://doi: 10.1016/j.mcat.2017.12.006.

[9] Tang, Y., Xue, Y., Li, Z., Yan, T., Zhou, R., 2018. Heterogeneous synthesis of glycerol carbonate from glycerol and dimethyl carbonate catalyzed by LiCl / CaO. Journal of Saudi Chemical Society, https://doi: 10.1016/j.jscs.2018.11.003.

[10] Qing, Y., Lu, H., Liu, Y., Liu, C., Liang, B., Jiang, W., 2018. Chinese Journal of Chemical Engineering Production of glycerol carbonate using crude glycerol from biodiesel production with DBU as a catalyst ☆. Chinese Journal of Chemical Engineering 26(9): 1912–9, https://doi: 10.1016/j.cjche.2018.01.010.

[11] Elhaj, E., Wang, H., Gu, Y., 2019. Functionalized quaternary ammonium salt ionic liquids (FQAILs) as an economic and e ffi cient catalyst for synthesis of glycerol carbonate from glycerol and dimethyl carbonate. Molecular Catalysis 468(February): 19–28, https://doi: 10.1016/j.mcat.2019.02.005.

[12] Wang, S., Hao, P., Li, S., Zhang, A., Guan, Y., Zhang, L., 2017. Applied Catalysis A , General Synthesis of glycerol carbonate from glycerol and dimethyl carbonate catalyzed by calcined silicates. Applied Catalysis A, General 542(January): 174–81, https://doi: 10.1016/j.apcata.2017.05.021.

[13] Li, Y., Liu, J., He, D., 2018. Applied Catalysis A , General Catalytic synthesis of glycerol carbonate from biomass-based glycerol and dimethyl carbonate over Li-La 2 O 3 catalysts. Applied Catalysis A, General 564(April): 234–42, https://doi: 10.1016/j.apcata.2018.07.032.

[14] Magniont, C., Escadeillas, G., Oms-multon, C., Caro, P. De., 2010. Cement and Concrete Research The bene fi ts of incorporating glycerol carbonate into an innovative pozzolanic matrix. Cement and Concrete Research 40(7): 1072–80, https://doi: 10.1016/j.cemconres.2010.03.009.

[15] Valentin, R., Alignan, M., Giacinti, G., Renaud, F.N.R., Raymond, B., Mouloungui, Z., 2012. Journal of Colloid and Interface Science Pure short-chain glycerol fatty acid esters and glycerylic cyclocarbonic fatty acid esters as surface active and antimicrobial coagels protecting surfaces by promoting superhydrophilicity. Journal of Colloid And Interface Science 365(1): 280–8, https://doi: 10.1016/j.jcis.2011.09.010.

[16] Yoo, J., Mouloungui, Z., 2003. Catalytic carbonylation of glycerin by urea in the presence of zinc mesoporous system for the synthesis of glycerol carbonate. Surface Science and Catalysis (6): 757–60.

[17] Aresta, M., Dibenedetto, A., Nocito, F., Pastore, C., 2006. A study on the carboxylation of glycerol to glycerol carbonate with carbon dioxide : The role of the catalyst , solvent and reaction conditions. Molecular Catalysis A 257: 149–53, https://doi: 10.1016/j.molcata.2006.05.021.

[18] Fujita, S.I., Yamanishi, Y., Arai, M., 2013. Synthesis of glycerol carbonate from glycerol and urea using zinc-containing solid catalysts: A homogeneous reaction. Journal of Catalysis, https://doi: 10.1016/j.jcat.2012.10.001.

[19] Kondawar, S.E., Mane, R.B., Vasishta, A., More, S.B., Dhengale, S.D., Rode, C. V., 2017. Carbonylation of glycerol with urea to glycerol carbonate over supported Zn catalysts. Applied Petrochemical Research, https://doi: 10.1007/s13203-017-0177-2.

[20] Cheol, S., Hwan, Y., Lee, H., Young, D., Keun, B., 2007. Lipase-catalyzed synthesis of glycerol carbonate from renewable glycerol and dimethyl carbonate through transesterification 49: 75–8, https://doi: 10.1016/j.molcatb.2007.08.007.

[21] Climent, M.J., Corma, A., Frutos, P. De., Iborra, S., Noy, M., Velty, A., et al., 2010. Chemicals from biomass : Synthesis of glycerol carbonate by transesterification and carbonylation with urea with hydrotalcite catalysts . The role of acid – base pairs. Journal of Catalysis 269(1): 140–9, https://doi: 10.1016/j.jcat.2009.11.001.

[22] Wang, L., Ma, Y., Wang, Y., Liu, S., Deng, Y., 2011. Efficient synthesis of glycerol carbonate from glycerol and urea with lanthanum oxide as a solid base catalyst. Catalysis Communications 12(15): 1458–62, https://doi: 10.1016/j.catcom.2011.05.027.

[23] Mu, J., D, P., 1981. Thermal Decomposition Of Carbonates, Carboxylates, Oxalates, Acetates, Formates, and Hydroxides. Acfa, Thermochimica 49: 207–18.

[24] Chen, C., Liu, P., Lu, C., 2008. Synthesis and characterization of nano-sized ZnO powders by direct precipitation method. Chemical Engineering Journal 144(3): 509–13, https://doi: 10.1016/j.cej.2008.07.047.

[25] Alim, K.A., Fonoberov, V.A., Shamsa, M., Balandin, A.A., Alim, K.A., Fonoberov, V.A., et al., 2005. Micro-Raman investigation of optical phonons in ZnO nanocrystals Micro-Raman investigation of optical phonons in ZnO nanocrystals. AIP Journal of Applied Physics 124313, https://doi: 10.1063/1.1944222.

[26] Guerfi, K., Lagerge, S., Meziani, M.J., Nedellec, Y., Chauveteau, G., 2005. Influence of the oxidation on the surface properties of silicon carbide. Thermochimica Acta 434: 140–9, https://doi: 10.1016/j.tca.2005.01.038.

[27] Hammond, C., Lopez-Sanchez, J.A., Mohd Hasbi Ab Rahim, N.D., Jenkins, R.L., Carley, A.F., He, Q., et al., 2011. Synthesis of glycerol carbonate from glycerol and urea with gold-based catalysts. Dalton Transaction 40: 3761–996, https://doi: 10.1039/C0DT01688H.

[28] Zoubida, L., Hichem, B., n.d. The The Nanostructure Nanostructure Zeolites Zeolites MFI-Type. Intech Open, https://doi: 10.5772/intechopen.77020.

[29] Gong, T., Qin, L., Lu, J., Feng, H., 2015. ZnO modified ZSM-5 and Y zeolites fabricated by atomic layer deposition for propane conversion †. Physical Chemistry 18: 601–14, https://doi: 10.1039/C5CP05043J.

[30] Aresta, M., Dibenedetto, A., Nocito, F., Ferragina, C., 2009. Valorization of bio-glycerol : New catalytic materials for the synthesis of glycerol carbonate via glycerolysis of urea. Journal of Catalysis 268(1): 106–14, https://doi: 10.1016/j.jcat.2009.09.008.